Chemical Physics Letters 481 (2009) 118–123

Contents lists available at ScienceDirect

Chemical Physics Letters

journal homepage: www.elsevier.com/locate/cplett

Concerted quantum effects of electronic and nuclear fluxes in molecules

Ingo Barth [a], Hans-Christian Hege [b], Hiroshi Ikeda [c], Anatole Kenfack [a], Michael Koppitz [b], Jörn Manz [a,*], Falko Marquardt [b], Guennaddi K. Paramonov [a]

[a] Institut für Chemie und Biochemie, Freie Universität Berlin, 14195 Berlin, Germany
[b] Visualization and Data Analysis, Zuse Institute Berlin, 14195 Berlin, Germany
[c] Department of Applied Chemistry, Graduate School of Engineering and The Research Institute for Molecular Electronic Devices, Osaka Prefecture University, Sakai, Osaka 599-8531, Japan

ARTICLE INFO

Article history:
Received 13 May 2009
In final form 2 September 2009
Available online 6 September 2009

ABSTRACT

Common myth suggests synchronicity and unidirectionality of nuclear and electronic fluxes. Accurate quantum dynamics simulations of the vibrating model system, aligned H_2^+, confirm this rule, but with exceptional opposite behaviours during short periods in the attosecond time domain. The ratio of electronic versus nuclear fluxes increases systematically, from small to large amplitude nuclear motions. Visualization of the electronic and nuclear densities and flux densities reveals that this is due to broader dispersion of electronic wavepackets compared to nuclear ones. The accurate results validate an efficient general method for quantum calculations of the fluxes in terms of densities, not flux densities.

1. Introduction

Chemical reactions and molecular vibrations involve simultaneous fluxes of the coupled nuclei (F_{nu}) and electrons (F_{el}) in molecules. The individual fluxes F_{nu} and F_{el} have been investigated previously, but so far without any quantum evaluations of concerted effects. On one hand, for example, nuclear fluxes through a dividing surface which separates the domains associated with the reactants and products, typically close to the transition state, determine the rates of chemical reactions. Quantum expressions of the corresponding nuclear (*nu*) flux operator [1–3] allow ab initio calculations of reaction rates [4,5]. The fluxes (also called 'currents') have dimensions of $1/time$; they may be evaluated as surface integrals over nuclear flux densities $\mathbf{j}_{nu}$ (also called 'current densities' or 'probability current densities') which have dimensions of $1/(time \times area)$; moreover, the time integral of the nuclear flux gives the yield Y_{nu} of the reaction. On the other hand, organic, inorganic, and biochemists have developed and applied powerful albeit less quantitative rules for electronic fluxes which accompany the nuclear motions [6–15]. These allow efficient predictions of the reactions – but quantum mechanics has never been applied to investigate the related questions such as: how many electrons are actually travelling with the nuclei? What is the ratio of the electronic versus nuclear fluxes? Are they flowing synchronously? On which time scale? In which direction?

As an example, consider pericyclic reactions such as the Cope rearrangement of 1,5-hexadiene or derivatives – a prototype is sketched in Fig. 1: Depending on substituents, various possible fluxes of one or two electrons are indicated by single and double-headed arrows, respectively, allowing to predict the breaking and the making of chemical bonds, together with associated transitions from single to double bonds, or vice versa. But the preceding questions about these fluxes lead into *terra incognita*. Our motivation to answer them has been stimulated by recent experimental observations and quantum simulations of the motions of electrons and nuclei in real time, with time resolutions from few tens of attoseconds ($1as = 10^{-18}$ s) to femtoseconds ($1\ fs = 10^{-15}$ s) [16–21]. To the best of our knowledge, the simultaneous electronic and nuclear fluxes in molecules, however, have never been evaluated or analyzed quantum mechanically even though one may anticipate that they should be an ubiquitous phenomenon. Very recently, Okuyama and Takatsuka have introduced a complex-valued electron flux density, with imaginary and real parts which are called the adiabatic and induced flux densities, respectively. Their approach reveals information of dynamical electron flows from adiabatic (i.e. based on the Born–Oppenheimer ansatz) electronic wavefunctions calculated in the frame of the so-called ab initio molecular dynamics, i.e. classical not quantum nuclear dynamics, as well as semiclassical Ehrenfest theory [22].

The purpose of this Letter is threefold: (a) To develop and validate a general approximate quantum method which allows to evaluate the simultaneous fluxes of electrons and nuclei in molecules. (b) To answer the preceding questions for a model system. (c) To present the first visualization of the underlying electronic and nuclear flux densities, together with their densities. In particular, we are interested in quantifying these processes in the electronic ground state, the domain of most thermal chemical processes. The method should be entirely general, however, e.g. it should also allow to describe electronic and nuclear fluxes in coupled

* Corresponding author. Fax: +49 30 838 54792.
E-mail address: jmanz@chemie.fu-berlin.de (J. Manz).

0009-2614/$ - see front matter © 2009 Elsevier B.V. All rights reserved.
doi:10.1016/j.cplett.2009.09.011

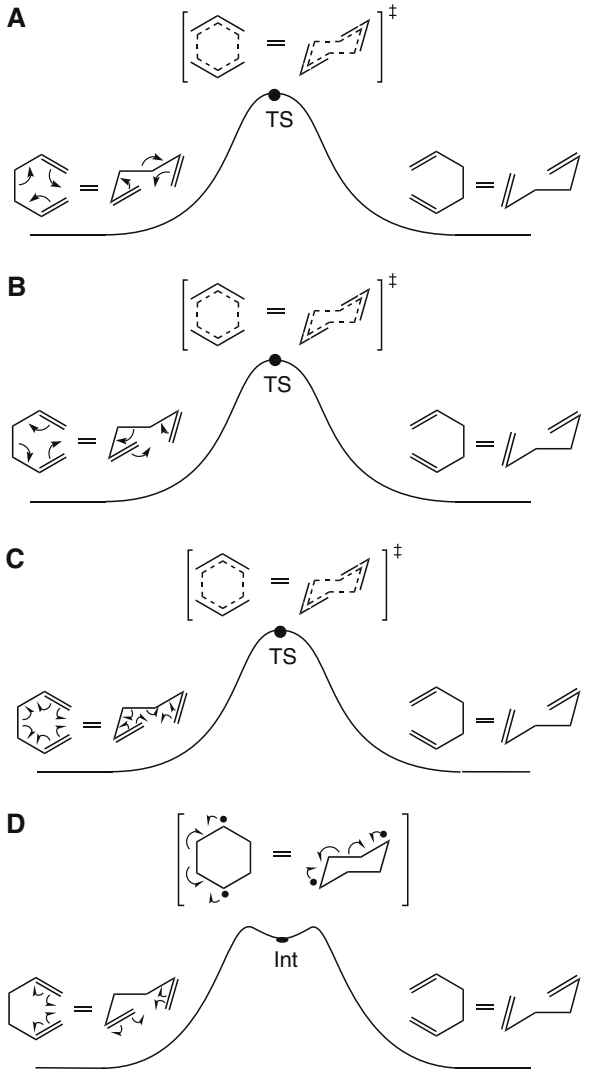

Fig. 1. Motivation of the present investigation from organic chemistry [6–11]: electron fluxes of one or two electrons are indicated by curved single or double-headed arrows, respectively. The example shows the controversial reaction mechanism of the Cope rearrangement of 1,5-hexadiene or derivatives, depending on substitution. (panels A–C) Plausible concerted mechanisms via the transition state (TS) with various electron fluxes. (panel D) A putative stepwise mechanism via a cyclohexa-1,4-diyl intermediate (Int). The arrows do not provide any information about the synchronicity, directionality, the time scale or magnitude of the fluxes, calling for our new approach.

electronic excited states, the domain of photochemistry. Moreover, it should allow for applications of arbitrary external fields. For reference, we investigate the fluxes associated with small and large amplitude vibrations in H_2^+ as our model system, because this allows to compare the results of the approximate method with accurate quantum dynamics simulations. State-of-the-art methods for accurate quantum computations (i.e. without any approximations such as softcore potentials, or restricted dimensionalities) of nuclear *and* electronic dynamics allow to consider only processes in very small systems as touchstone for the new approximate method, supporting extensions to larger molecules. Recently, complementary investigations of the systems H_2^+, H_2, or isotopomers, have already discovered fascinating details of the coupled electronic and nuclear dynamics, but without considerations of concerted electronic and nuclear fluxes [16,18–20,23,24]. Nevertheless, the resulting yields of dissociation and ionization of the laser driven model systems, H_2^+ and HD^+, have been evaluated quantum mechanically, by integration of the coupled nuclear and electronic quantum flux densities [23].

2. Theory and model

Our derivation starts with the time-dependent Schrödinger equation for non-relativistic processes in molecules in the laboratory frame [25],

$$i\hbar\frac{\partial}{\partial t}\Psi(\mathbf{q},\mathbf{Q},t)=\mathscr{H}(\mathbf{q},\mathbf{Q})\Psi(\mathbf{q},\mathbf{Q},t), \tag{1}$$

where $\mathscr{H}(\mathbf{q},\mathbf{Q})$ denotes the molecular Hamiltonian, depending on $\mathbf{Q}$ and $\mathbf{q}$, i.e. the spatial and spin coordinates of N_{nu} nuclei $\mathbf{Q}_k=\{\mathbf{R}_k,\Sigma_k\}$ $(k=1,\ldots,N_{nu})$ and of N_{el} electrons $\mathbf{q}_l=\{\mathbf{r}_l,\sigma_l\}$ $(l=1,\ldots,N_{el})$. The Hamiltonian may include external fields – important applications include scenarios where the molecular center of mass has been centered at the origin, and the molecule is aligned or oriented in the laboratory. The wavefunction $\Psi(\mathbf{q},\mathbf{Q},t)$ of the entire system should be antisymmetric for the electrons and for indistinguishable nuclei with half integer nuclear spins, and symmetric for distinguishable nuclei with integer spins. Extensions to Hamiltonians $\mathscr{H}(\mathbf{q},\mathbf{Q},t)$ describing interactions with time-(t)-dependent external fields will be considered elsewhere. The complex wavefunction $\Psi(\mathbf{q},\mathbf{Q},t)$ allows to calculate the $N_{nu}+N_{el}$ particle density $\rho(\mathbf{q},\mathbf{Q},t)=|\Psi(\mathbf{q},\mathbf{Q},t)|^2$ and flux density $\mathbf{j}(\mathbf{q},\mathbf{Q},t)$ of the entire system, satisfying the continuity equation

$$\dot{\rho}(\mathbf{q},\mathbf{Q},t)=-\mathbf{div}\,\mathbf{j}(\mathbf{q},\mathbf{Q},t) \tag{2}$$

in accord with the Schrödinger equation, Eq. (1). Here, $\mathbf{j}(\mathbf{q},\mathbf{Q},t)$ and **div** denote a vector and the corresponding operator for the derivative, with $3(N_{nu}+N_{el})$ components, respectively. By integrating ρ and $-\mathbf{div}\,\mathbf{j}$ over all coordinates complementary to $\mathbf{r}=\mathbf{r}_l$ or $\mathbf{R}=\mathbf{R}_k$, one obtains the electronic and nuclear one-particle densities $\rho_{el}(\mathbf{r},t)$ and $\rho_{nu,k}(\mathbf{R},t)$ as well as the derivatives of the flux densities $\mathbf{j}_{el}(\mathbf{r},t)$ and $\mathbf{j}_{nu,k}(\mathbf{R},t)$, respectively. Since the nuclear distributions change during any chemical reaction or coherent vibration, it follows that the one-particle densities and flux densities are all time-dependent. In particular, any changes in the nuclear wavefunction will, of course, induce changes in the one-electron density. The fundamental continuity equation, Eq. (2), implies the corresponding one-particle continuity equations

$$\dot{\rho}_{el}(\mathbf{r},t)=-\nabla_{\mathbf{r}}\cdot\mathbf{j}_{el}(\mathbf{r},t) \tag{3}$$

$$\dot{\rho}_{nu,k}(\mathbf{R},t)=-\nabla_{\mathbf{R}}\cdot\mathbf{j}_{nu,k}(\mathbf{R},t) \tag{4}$$

for the electrons and nuclei, respectively.

Before we proceed to derive the expressions for the corresponding electronic and nuclear fluxes, let us first consider the difficulty which would be implied in case of direct use of Eqs. (3) and (4) in the frame of the celebrated Born–Oppenheimer (BO) approximation which is based on the huge difference of the nuclear and electronic masses [26]. Accordingly, the molecular Hamiltonian, $\mathscr{H}(\mathbf{q},\mathbf{Q})=\mathscr{T}_{nu}+\mathscr{H}_{el}(\mathbf{q};\mathbf{Q})$ contains the nuclear kinetic energy $\mathscr{T}_{nu}$, and the complementary, so-called electronic Hamiltonian $\mathscr{H}_{el}(\mathbf{q};\mathbf{Q})$ for the electronic kinetic energy as well as the Coulomb interactions of all particles. The latter depends parametrically on $\mathbf{Q}$; subsequently we neglect spin–orbit interactions. The wavefunction for electrons and nuclei in the electronic ground state is then approximated as

$$\Psi_{BO}(\mathbf{q},\mathbf{Q},t)=\Psi_{BO,nu}(\mathbf{Q},t)\times\Psi_{BO,el}(\mathbf{q};\mathbf{Q}), \tag{5}$$

where $\Psi_{BO,nu}$ and $\Psi_{BO,el}$ denote the normalized time-dependent nuclear and time-independent electronic wavefunctions, respectively. Specifically, $\Psi_{BO,el}$ is calculated as *real* solution of the time-independent electronic Schrödinger equation

$$\mathscr{H}_{el}(\mathbf{q};\mathbf{Q})\Psi_{BO,el}(\mathbf{q};\mathbf{Q})=V_{el}(\mathbf{Q})\Psi_{BO,el}(\mathbf{q};\mathbf{Q}), \tag{6}$$

together with the (adiabatic, ground state) potential energy surface $V_{el}(\mathbf{Q})$, whereas $\Psi_{BO,nu}(\mathbf{Q},t)$ is the *complex* solution of the time-dependent nuclear Schrödinger equation

$$ih\frac{d}{dt}\Psi_{BO,nu}(\mathbf{Q},t) = (\mathscr{T}_{nu} + V_{el}(\mathbf{Q}))\Psi_{BO,nu}(\mathbf{Q},t). \quad (7)$$

For calculations of time-independent molecular properties, separation of the variables t and $\mathbf{Q}$ yields stationary nuclear wavefunctions $\Psi_{BO,nu}(\mathbf{Q})$, together with corresponding rotational and vibrational energies in the electronic ground state, depending on nuclear quantum numbers. Extensions to coupled electronic ground and excited states yield the BO expansion of the total wavefunction in corresponding products of nuclear and electronic wavefunctions [27].

For nearly a century, quantum chemists focussed on solving the electronic Schrödinger equation, Eq. (6), with milestones which have been recognized last but not least by the awards of Nobel prizes to several pioneers, till today's highly advanced state-of-the-art. It is thus fair to say that Dirac's vision [28] that the fundamental Eq. (1) describes the whole of (non-relativistic) chemistry has become reality, concerning the calculation of the time-independent properties of molecules in the electronic ground state, by means of the BO wavefunctions $\Psi_{BO,el}(\mathbf{q};\mathbf{Q})$ and $\Psi_{BO,nu}(\mathbf{Q})$. More recently, the field of nuclear quantum dynamics has also seen stupendous advances in the computations of $\Psi_{BO,nu}(\mathbf{Q},t)$ for the nuclear motions of large molecules [5,29,30].

In contrast with the rather mature fields of quantum chemistry for stationary molecular properties and of quantum reaction dynamics for nuclear motions, accurate evaluations of the general Schrödinger equation, Eq. (1), for electrons *and* nuclei are still restricted to the smallest systems, vide infra [16,18–20,23,24]. First extensions to larger molecules have been suggested in Refs. [31,32], but quantum evaluations of the flux densities $\mathbf{j}$ and the resulting simultaneous nuclear and electronic flux densities $\mathbf{j}_{nu,k}(\mathbf{R},t)$ and $\mathbf{j}_{el}(\mathbf{r},t)$, Eqs. (3) and (4), have not been carried out. Several previous attempts to develop approximate quantum methods for electronic flux densities are documented in Refs. [22,33–35]. All of them conclude that the task is very difficult. For reference, they note that the BO approximation, Eq. (5), which is so powerful concerning time-independent properties as well as nuclear dynamics, fails completely concerning time-dependent electronic flux densities, i.e.

$$\mathbf{j}_{BO,el}(\mathbf{r},t) = \mathbf{0}, \quad (8)$$

because the electronic wavefunctions $\Psi_{el}(\mathbf{q};\mathbf{Q})$ in electronic non-degenerate states are *real*. On first glance, it would thus appear to be helpless to employ the BO approximation for calculations of electronic fluxes – Born and Oppenheimer focussed on stationary properties of molecules, not on time-dependent fluxes! Some important exceptions from Eq. (8) have been discovered recently, i.e. strong electronic ring currents or electron circulations exist, even in BO approximation, in symmetric (e.g. ring-shaped or linear) [36–38] or nearly symmetric [39] molecules which support degenerate *complex* electronic excited states, see also the related experimental investigation [40]. We note in passing that analogous nuclear ring currents exist in symmetric (e.g. linear) molecules which support degenerate *complex* pseudorotational states [41]. But for coherent vibrations and chemical reactions in non-degenerate *real* electronic states, it appeared that one has to go beyond the BO approximation in order to overcome its fundamental failure, Eq. (8) [22,33–35].

In contrast with all previous approaches, we note that, for the purpose of this Letter, it is not even necessary to calculate the electronic and nuclear flux densities, i.e. all that we need in order to answer the questions about the electronic and nuclear fluxes F_{el} and $F_{nu,k}$ is to calculate the net integrals of the corresponding flux densities, e.g.

$$F_{el}(t;A_{obs}) = -\int_{A_{obs}} d\mathbf{A}\cdot\mathbf{j}_{el}(\mathbf{r},t) \quad (9)$$

for electrons. In Eq. (9), A_{obs} denotes a surface (with unit normal vector $\mathbf{n}$, i.e. $d\mathbf{A}=\mathbf{n}\,dA$) of an 'observer' (*obs*), who monitors and integrates the flux density of the electrons which pass through the surface. We shall now show that F_{el} can also be calculated using the electronic density $\rho_{el}(\mathbf{r},t)$, instead of the flux density $\mathbf{j}_{el}(\mathbf{r},t)$. For this purpose, we note that electronic fluxes are zero at infinity. This allows us to rewrite Eq. (9) using Gauss's theorem and the continuity equation, Eq. (3), as

$$F_{el}(t;A_{obs}) = -\int_{V_{obs}} dV\nabla_r\cdot\mathbf{j}_{el}(\mathbf{r},t) = \frac{d}{dt}\int_{V_{obs}} dV\rho_{el}(\mathbf{r},t) \quad (10)$$

where V_{obs} denotes the part of the total volume (V) which is located on one side of the dividing surface A_{obs}, with the surface vector $d\mathbf{A}_{obs}$ pointing away from V_{obs}. Eq. (10) is a key result of this Letter. The time integration of the net electronic flux, Eq. (10), leads to the yield $Y_{el}(t;A_{obs})$ of electrons which pass through the surface of the observer from the initial ($t_i = 0$) till the final ($t_f = t$) times,

$$Y_{el}(t;A_{obs}) = \int_{V_{obs}} dV\rho_{el}(\mathbf{r},t) - \int_{V_{obs}} dV\rho_{el}(\mathbf{r},0). \quad (11)$$

Note that $Y_{el}(t;A_{obs})$ can be positive or negative, depending on the directionality of the flux. Turning the table, we obtain the net electronic flux F_{el}, Eq. (10), as the time derivative of the yield (11), i.e. in terms of $\rho_{el}(\mathbf{r},t)$, instead of $\mathbf{j}_{el}(\mathbf{r},t)$.

Since we know from quantum chemistry that the BO separation provides excellent approximations of the electronic densities, we now suggest to use the BO approximation for the electronic density $\rho_{BO,el}(\mathbf{r},t)$ in Eqs. (10) and (11) to obtain the net electronic flux $F_{BO,el}(t;A_{obs})$ and the net electronic yield $Y_{BO,el}(t;A_{obs})$, respectively.

Analogous derivations apply for the nuclei. The resulting expressions are

$$F_{nu,k}(t;A_{obs}) = -\int_{A_{obs}} d\mathbf{A}\cdot\mathbf{j}_{nu,k}(\mathbf{R},t) = \frac{d}{dt}\int_{V_{obs}} dV\rho_{nu,k}(\mathbf{R},t) \quad (12)$$

for the net nuclear flux through the surface of the 'observer' and

$$Y_{nu,k}(t;A_{obs}) = \int_{V_{obs}} dV\rho_{nu,k}(\mathbf{R},t) - \int_{V_{obs}} dV\rho_{nu,k}(\mathbf{R},0) \quad (13)$$

for the nuclear yield. The corresponding BO approximations for the nuclear flux and yield are obtained using Eqs. (12) and (13) with density of the nucleus k at time t in BO approximation, $\rho_{BO,nu,k}(\mathbf{R},t)$.

The general expressions Eq. (10) and (12) with the electronic and nuclear BO densities are the suggested approximations for the electronic and nuclear fluxes, respectively. We call them 'BO approximations', because they employ the BO densities, irrespective of the failure of the BO approximation, Eq. (8).

For the application of the BO approximation to the nuclear and electronic fluxes in vibrating H_2^+ and comparison with accurate results, we assume that the molecule has been aligned along the Z-axis, with its center of mass at the origin, such that the nuclei are distinguishable, e.g. using the method of Refs. [38,42]. The coupled electron and nuclear dynamics is evaluated in terms of Jacobi coordinates for the internuclear distance R and the vector $\mathbf{r}$ from their center of mass to the electron, represented in terms of cylindrical coordinates $\{z,\rho,\phi\}$. Accordingly, the nuclear coordinates are given, in excellent approximation, by $Z_1 = -Z_2 = R/2$. Details of the transformation from the preceding laboratory-fixed coordinates $\{\mathbf{r},\mathbf{R}_1,\mathbf{R}_2\}$ to the molecule-fixed ones $\{z,\rho,\phi,R\}$ (subject to the constraints of fixed center of mass and orientation) will be presented elsewhere. We assume that initially, the system has been stretched in order to induce coherent vibrations. One can induce small to large amplitude vibrations, depending on the initial stretch

$\langle R(t=0)\rangle$, e.g. using the methods of Refs. [43–46] – the challenge is to evaluate the electronic fluxes which accompany the nuclear ones; systematic effects of variations of $\langle R(t=0)\rangle$ will be discussed in the next section. Specifically, the initial wavefunction is constructed as BO wavefunction $\Psi_{BO,nu,v=0}(R)\times\Psi_{BO,el}(z,\rho,\phi;R)$ for the electronic and vibrational ground state ($^2\Sigma_g^+(v=0)$), with the center of its nuclear wavefunction shifted from $\langle R\rangle_{v=0}=R_e$ to $\langle R(t=0)\rangle$, i.e. the initial amplitude of nuclear vibration is $\Delta R(t=0)=\langle R(t=0)\rangle-\langle R\rangle_{v=0}$. The time-dependent BO wavefunction $\Psi_{BO}(z,\rho,\phi,R,t)=\Psi_{BO,nu}(R,t)\times\Psi_{BO,el}(z,\rho,\phi;R)$ (together with the potential energy curve $V_{^2\Sigma_g^+}(R)$), is obtained as product of the solutions of the corresponding electronic and nuclear Schrödinger equations, using standard techniques. For comparison, the accurate wavefunction $\Psi(z,\rho,\phi,R,t)$ starts from the same initial wavefunction, which is then propagated as solution of the time-dependent Schrödinger equation, Eq. (1), using the method of Ref. [23], with corresponding grid representation for the variables $\{z,\rho,R\}$, and exploiting the cylindrical symmetry for ϕ. The same grid is used for the BO approximation. Further technical details will be reported elsewhere. Exemplarily, two surfaces A_{obs} of observers are defined as horizontal planes parallel to the x–y plane, at symmetric distances $Z_{obs}=\pm R_{obs}/2$, cf. Fig. 2, where R_{obs} is half way between the maximum and minimum mean bond length $\langle R(t)\rangle$: This choice is made because this is where we expect to monitor the largest possible nuclear fluxes. In contrast, we anticipate negligible nuclear fluxes close to the turning points, $\max\langle R(t)\rangle$ and $\min\langle R(t)\rangle$. This working hypothesis is confirmed by the results for $\langle R(t)\rangle$ and $F_{nu,k}(t;A_{obs})$ $(k=1,2)$, cf. Fig. 2a and b, respectively. Note that $\min\langle R(t)\rangle$ is significantly larger than the classical turning point, due to substantial dispersion of the wavepacket. The volume V_{obs} is the domain $Z>Z_{obs}$.

3. Results and discussion

Applications of the theory for electronic and nuclear fluxes which accompany molecular dynamics are demonstrated in Fig. 2, exemplarily for coherent vibrations of aligned H_2^+. As first case, consider the scenario $\langle R(t=0)\rangle=2R_e$, where $R_e=2a_0$ is the

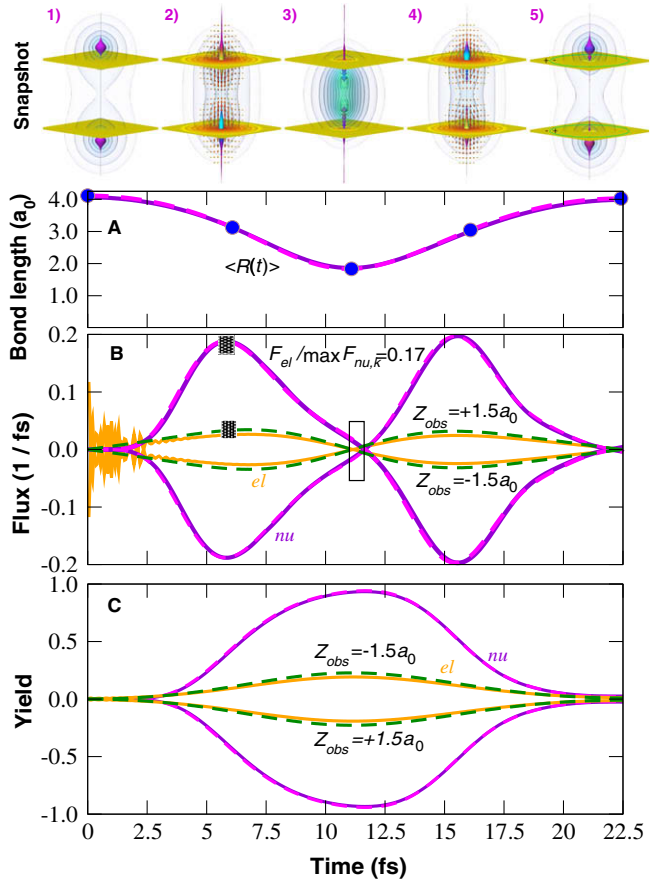

Fig. 2. Nuclear ('*nu*') and electronic ('*el*') fluxes through two planes of observers located at $Z_{obs}=+1.5a_0$ and $Z_{obs}=-1.5a_0$ (panel B) and yields (panel C) during large amplitude vibration of H_2^+ in the electronic ground state $^2\Sigma_g^+$ (panel A), with comparison of accurate (continuous lines) results and the present Born–Oppenheimer approximation (dashed lines). The underlying changes of the electronic and nuclear densities as well as the flux densities are visualized *simultaneously* (top row with five snapshots); for a blow-up and the color codes, see Fig. 3. Panel A: mean bond distance $\langle R(t)\rangle$, starting from amplitude $\langle R(0)\rangle=2R_e=4a_0$; the snapshots are taken where indicated. Panel B: The ratio of the fluxes $F_{el}/\max F_{nu,k}=0.17$ is determined where indicated. Electronic and nuclear fluxes are opposite during the attosecond time interval marked by the empty box.

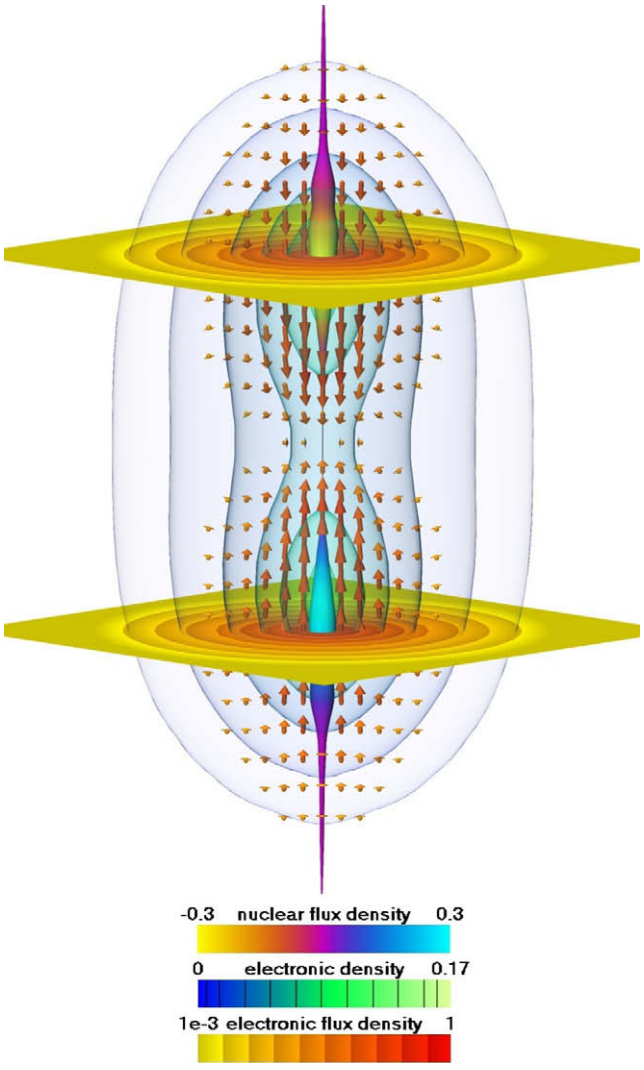

Fig. 3. Blow-up of second snapshot, shown in the top panel of Fig. 2 ($t=6.45$ fs) – visualizing simultaneously nuclear and electronic densities as well as flux densities, with color codes as indicated. The following is valid also for all snapshots displayed in Fig. 2: The magnitude of the nuclear density is proportional to the radius of the rotationally symmetric shape around the H_2^+ symmetry axis; the magnitude and direction of the nuclear flux density are color coded on this shape, cf. 'nuclear flux density' color map. The electronic density is displayed using nested, semi-transparent isosurfaces; they are colored according to the 'electronic density' color map; the lines in the color map indicate the chosen iso-levels. The electronic flux density is depicted by the vectors and by the contours in the two observer planes using the same logarithmic 'electronic flux density' color map.

equilibrium distance, cf. Fig. 2a. Obviously, the agreement of the accurate results and the BO approximation is in general excellent, not only for the mean bond length (panel 2a) but also for the electronic and nuclear fluxes (panel 2b) and the yields (panel 2c). The only discrepancy is seen for the initial time evolution (less than 3 fs) where the accurate electronic flux $F_{el}(t;A_{obs})$ shows high-frequency oscillations which are absent in $F_{BO,el}(t;A_{obs})$. This is a numerical artifact implied by the initial BO wavefunction – the accurate solution reproduces this as a superposition of the dominant electronic ground state and a very small component of the electronic excited state, with the same $(^2\Sigma_g^+)$ symmetry. Accordingly, the oscillatory frequency times $\hbar$ correspond to the potential energy gap between the electronic ground and excited state, close to the initial bond length $\langle R(0)\rangle$ [47]. Soon after this initialization, the nuclear wavefunctions in the electronic ground and excited states move towards smaller and larger bond lengths, respectively, i.e. they can no longer overlap, such that the artificial oscillatory patterns in $F_{el}(t;A_{obs})$ vanish within ≈ 3 fs, in accord with Ref. [48].

Fig. 2a and b (together with Figs. 3 and 4, see below) discover all the answers to the questions at the beginning of this Letter, for the present example of the aligned H_2^+. To begin, the symmetry of the system implies the corresponding symmetry of the fluxes, i.e. the directions of the electronic and nuclear fluxes through the parallel planes of the observers at $Z_{obs} = \pm R_{obs}/2$. Specifically, for most of the time, the directions of the nuclear fluxes are along the nuclear momenta, or equivalently along the time derivatives of the nuclear coordinates $\langle \dot{Z}_1(t)\rangle = -\langle \dot{Z}_2(t)\rangle \approx \langle \dot{R}(t)\rangle/2$, of the two nuclei $(k = 1, 2)$, compare Fig. 2a and b. Also, for most of the time, the electronic fluxes $F_{el}(t;A_{obs})$ follow the nuclear ones $F_{nu,k}(t;A_{obs})$. This is in accord with an intuitive hypothesis which underlies the BO approximation, i.e. the light electrons can adapt to the motions of the heavy nuclei quasi-instantaneously. The overall time scale of the nuclear and electronic fluxes is, therefore, similar to the vibrational period. Surprisingly, however, Fig. 2b also reveals exceptions from this rule of the unidirectionality of nuclear and electronic fluxes: In particular, there are short time intervals with opposite directions of the nuclear and electronic fluxes, typically when they switch directionality within less than 1 fs. This is due not only to the different dispersions of the nuclear and the electronic wavepackets, but also to the corresponding densities and flux densities which are illustrated by means of snapshots, in the top of Fig. 2, see also the blow-up in Fig. 3. Note that this is the first visualization of both nuclear and electronic flux densities, together with the two densities. These accurate quantum results have been evaluated using the method of Ref. [23]; in contrast, the BO approximation is not applicable for this purpose (Eq. (8), $\mathbf{j}_{BO,el} = 0$).

Another concerted quantum effect of the fluxes is discovered in Fig. 2c. Apparently the nuclear yields reach maximum (minimum) values close to 1 (−1), i.e. the nuclei travel almost completely from initial locations corresponding to large bond distances $\langle R(0)\rangle$ to short ones $\min\langle R(t)\rangle$, and back. The small deviation from ideal values 1 (−1) are due to the dispersions of the nuclear wavepackets. In contrast, only about $2 \times 22 = 44\%$ of the electron pass through the planes of the observers, in opposite directions. The much smaller absolute values of the electronic yields, compared to the nuclear ones, corresponds to the rather small value of the ratio $F_{el}(t;A_{obs})/\max F_{nu,k}(t;A_{obs}) = 0.17$, cf. Fig. 2b. This is a consequence of the much larger dispersion of the electronic wavepacket, compared to the nuclear one, cf. Fig. 3. Ultimately, this is due to the much smaller mass of the electron, compared to the nuclei.

Fig. 4 shows the results of a systematic investigation of the ratio of the magnitudes of the electronic versus maximum nuclear fluxes $F_{el}(t;A_{obs})/\max F_{nu,k}(t;A_{obs})$, depending on the initial amplitude $\Delta R = \langle R(0)\rangle - \langle R\rangle_{v=0}$ of vibration, with $\langle R\rangle_{v=0} = R_e = 2a_0$. Predominantly, small and large amplitude motions are associated with small or large ratios of electronic versus nuclear fluxes, respectively. This tells us that the electronic densities are quite robust for small amplitude vibrations, whereas large amplitude nuclear motions cause significant changes of the electronic wavepackets which travel with the nuclei. Intuitively, one would expect that the ratio $F_{el}(t;A_{obs})/\max F_{nu,k}(t;A_{obs})$ should approach the limit 1/2 (i.e. half of the electron is travelling with each of the nuclei) for very large amplitudes. The fact that this limit is not obtained in Fig. 4, even for quite large initial amplitudes ($\Delta R = 4a_0$) is due to another quantum effect, i.e. the vibration becomes slower than the dispersion of the wavepacket such that only about half of the molecule vibrates whereas the other half dissociates.

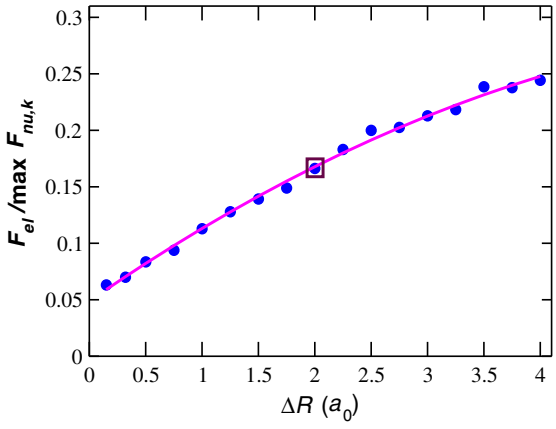

Fig. 4. Ratio of the magnitudes of the electronic and maximum nuclear fluxes $F_{el}/\max F_{nu,k}$ versus initial amplitude ΔR. The case of Fig. 2b is indicated by the square box.

4. Conclusion

This Letter achieves the triple goal:

(a) We have developed and validated a new, approximate quantum method for the coupled electronic and nuclear fluxes. The method bypasses the fundamental short-coming of the BO approximation concerning the electronic flux densities, Eq. (8), by means of Gauss's theorem as well as electronic and nuclear continuity equations, Eqs. (3) and (4), respectively. Gratifyingly, the final expressions, Eqs. (10) and (12), may also be written as time derivative of the electronic and nuclear mean values $d/dt\langle h\rangle_{el}$ and $d/dt\langle h\rangle_{nu}$ of the Heaviside function h which is equal to 1 (0) inside (outside) the volume V_{obs}, respectively. This is in formal analogy with corresponding mean values of Miller's flux operator $d/dt\,\hat{h}$ in the Heisenberg picture or $i/\hbar[\mathscr{H},\hat{h}]$ in the Schrödinger picture [3]; further details will be published elsewhere. They allow further extensions to several, possibly also non-planar dividing surfaces in order to investigate concerted fluxes of several electrons, associated with various nuclear fluxes during rearrangements of several bonds in molecules, in electronic ground and excited states. In any case, the coupled nuclear and electronic fluxes, and also the yields, are expressed no longer in terms of flux densities, but in terms of densities – this is the key to the present approximation which abandons the flux densities and employs the BO densities instead of accurate ones. The excellent agreement of the results of the accurate method [23] and the present BO approximation suggest to proceed to applications, from the 'touchstone' H_2^+ to large amplitude vibrations or reactions of polyatomic

molecules in all domains of chemistry. For this purpose, one can readily employ the arsenal of methods of quantum chemistry and quantum reaction dynamics, which has been developed over approximately 80 and 20 years, respectively. As byproduct, multiplication of the resulting fluxes and yields with the electronic and nuclear charges will also provide the associated electronic and nuclear currents and the transferred charges, respectively.

(b) The new method has allowed us to discover novel effects of the concerted nuclear and electronic fluxes. Most of the time, they confirm chemical intuition which underlies the BO approximation and which have become, indeed, dogmas since the original paper of Born and Oppenheimer [26], i.e. synchronicity and the same directionality of the nuclear and electronic fluxes. Surprisingly, however, we have also discovered exceptions from these rules, specifically during short periods (below 1 fs) when both the nuclear and electronic fluxes change directions. These effects deserve further investigations. Moreover, we could show that the electronic fluxes in H_2^+ are smaller than nuclear ones, due to larger dispersion of the wavefunctions $\Psi_{BO,el}(\mathbf{q};\mathbf{Q})$ of the light electrons compared to $\Psi_{BO,nu}(\mathbf{Q},t)$ of the heavy nuclei. The ratio of the magnitudes of the electronic versus nuclear fluxes increases systematically with the amplitude of nuclear motions. By extrapolation, this suggests a stimulating working hypothesis for many applications. For example, consider again the Cope rearrangement shown in Fig. 1: Contrary to the traditional rules [6–15], we anticipate that the electronic fluxes which are symbolized by the double headed arrows do not automatically represent fluxes of two electrons, e.g. they should be smaller for shaking single to double bonds, or vice versa, compared to making and breaking bonds. One should be able to measure these fluxes, e.g. using ultrafast photoelectron spectroscopy [49,50].

(c) Last but not least, we have presented the first visualization of the coupled nuclear and electronic densities and flux densities, see the snapshots in Figs. 2 and 3. Such visualization techniques provide new means for analysis and comprehension of the detailed mechanisms underlying the coupled nuclear and electronic fluxes.

This Letter should stimulate many applications to concerted effects of electronic and nuclear fluxes in molecules, as well as renewed efforts to derive related simple yet accurate expressions for the underlying flux densities.

Acknowledgement

We would like to express our gratitude to André D. Bandrauk (Sherbrooke), Dennis J. Diestler (Lincoln), E.K.U. Gross, Caroline Lasser, Gerd Multhaup, Beate Paulus, Hans-Ulrich Reissig, Wolfram Saenger (Berlin), Gernot Frenking (Marburg), Stefan Fischer, Peter Hofmann (Heidelberg), Hirohiko Kono (Sendai), Uwe Manthe (Bielefeld), William H. Miller (Berkeley), and Kazuo Takatsuka (Tokyo) for stimulating discussions and advice. Financial support by Freie Universität Berlin via the Center for Scientific Simulation, as well as by Deutsche Forschungsgemeinschaft, the Japan Society for the Promotion of Science, and by Fonds der Chemischen Industrie, is also gratefully acknowledged.

References

[1] W.H. Miller, J. Chem. Phys. 61 (1974) 1823.
[2] W.H. Miller, Acc. Chem. Res. 26 (1993) 174.
[3] W.H. Miller, J. Phys. Chem. A 102 (1998) 793.
[4] U. Manthe, T. Seideman, W.H. Miller, J. Chem. Phys. 101 (1994) 4759.
[5] T. Wu, H.-J. Werner, U. Manthe, Science 306 (2004) 2227.
[6] J.A. Berson, in: P. de Mayo (Ed.), Rearrangements in Ground and Excited States, vol. 1, Academic Press, New York, 1980, p. 311.
[7] T.H. Lowry, K.S. Richardson, Mechanism and Theory in Organic Chemistry, Harper and Row, New York, 1987.
[8] J.J. Gajewski, Hydrocarbon Thermal Isomerizations, Elsevier, Amsterdam, 2004.
[9] E.V. Anslyn, D.A. Dougherty, Modern Physical Organic Chemistry, University Science Books, Sausalito, 2006.
[10] M.B. Smith, J. March, Advanced Organic Chemistry Reactions, Mechanisms, and Structure, Wiley, Hoboken, 2007.
[11] K.P.C. Vollhardt, N.E. Schore, Organic Chemistry – Structure and Function, Freeman, New York, 2007.
[12] R.G. Wilkins, Kinetics and Mechanism of Reactions of Transition Metal Complexes, Verlag Chemie, Weinheim, 1991.
[13] R.B. Jordan, Reaction Mechanisms of Inorganic and Organometallic Systems, Oxford University Press, Oxford, 2007.
[14] C.K. Mathews, K.E. van Holde, K.G. Ahern, Biochemistry, Prentice-Hall, New Jersey, 1999.
[15] D.L. Nelson, M.M. Cox, Lehninger Principles of Biochemistry, Freeman, New York, 2009.
[16] A. Scrinzi, M.Y. Ivanov, R. Kienberger, D.M. Villeneuve, J. Phys. B 39 (2006) R1.
[17] P.B. Corkum, F. Krausz, Nature Phys. 3 (2007) 381.
[18] M.F. Kling et al., Science 312 (2006) 246.
[19] F. Martín et al., Science 315 (2007) 629.
[20] A.D. Bandrauk, S. Chelkowski, S. Kawai, H. Lu, Phys. Rev. Lett. 101 (2008) 153901.
[21] S.T. Park, A. Gahlmann, Y. He, J.S. Feenstra, A.H. Zewail, Angew. Chem. Int. Ed. 47 (2008) 9496.
[22] M. Okuyama, K. Takatsuka, Chem. Phys. Lett. 476 (2009) 109.
[23] G.K. Paramonov, Chem. Phys. Lett. 411 (2005) 350.
[24] H. Kono, Y. Sato, M. Kanno, K. Nakai, T. Kato, Bull. Chem. Soc. Jpn. 79 (2006) 196.
[25] E. Schrödinger, Ann. der Physik 81 (1926) 109.
[26] M. Born, R. Oppenheimer, Ann. der Physik 84 (1927) 457.
[27] D.J. Tannor, Introduction to Quantum Mechanics: A Time-Dependent Perspective, University Science Books, Sausalito, 2007.
[28] P.A.M. Dirac, Proc. Roy. Soc. London Ser. A 123 (1929) 714.
[29] G.A. Worth, H.-D. Meyer, H. Köppel, L.S. Cederbaum, I. Burghardt, Int. Rev. Phys. Chem. 27 (2008) 569.
[30] H.-D. Meyer, F. Gatti, G.A. Worth, Multidimensional Quantum Dynamics: MCTDH Theory and Applications, Wiley, Weinheim, 2009.
[31] L.S. Cederbaum, J. Chem. Phys. 128 (2008) 124101.
[32] D. Geppert, P. von den Hoff, R. de Vivie-Riedle, J. Phys. B 41 (2008) 074006.
[33] J.B. Delos, Rev. Mod. Phys. 53 (1981) 287.
[34] L.A. Nafie, J. Chem. Phys. 79 (1983) 4950.
[35] E. Deumeus, A. Diz, R. Longo, Y. Öhrn, Rev. Mod. Phys. 66 (1994) 917.
[36] I. Barth, J. Manz, Angew. Chem. Int. Ed. 45 (2006) 2962.
[37] I. Barth, J. Manz, Y. Shigeta, K. Yagi, J. Am. Chem. Soc. 128 (2006) 7043.
[38] I. Barth, L. Serrano-Andrés, T. Seideman, J. Chem. Phys. 129 (2008) 164303; I. Barth, L. Serrano-Andrés, T. Seideman, J. Chem. Phys. 130 (2009) 109901(E).
[39] M. Kanno, K. Hoki, H. Kono, Y. Fujimura, J. Chem. Phys. 127 (2007) 204314.
[40] M. Wollenhaupt, M. Krug, J. Köhler, T. Bayer, C. Sarpe-Tudoran, T. Baumert, Appl. Phys. B 95 (2009) 245.
[41] I. Barth, J. Manz, P. Sebald, Chem. Phys. 346 (2008) 89.
[42] H. Stapelfeldt, T. Seideman, Rev. Mod. Phys. 75 (2003) 543.
[43] B. Hartke, R. Kosloff, S. Ruhman, Chem. Phys. Lett. 158 (1989) 238.
[44] E. Goll, G. Wunner, A. Saenz, Phys. Rev. Lett. 97 (2006) 103003.
[45] Th. Ergler, B. Feuerstein, A. Rudenko, K. Zrost, C.D. Schröter, R. Moshammer, J. Ullrich, Phys. Rev. Lett. 97 (2006) 103004.
[46] W. Li, X. Zhou, R. Lock, S. Patchkovskii, A. Stolow, H.C. Kapteyn, M.M. Murnane, Science 322 (2008) 1207.
[47] S. Chelkowski, G.L. Yudin, A.D. Bandrauk, J. Phys. B 39 (2006) S409.
[48] A.D. Bandrauk, S. Chelkowski, P.B. Corkum, J. Manz, G.L. Yudin, J. Phys. B 42 (2009) 134001.
[49] A.D. Bandrauk, S. Chelkowski, H.S. Nguyen, Int. J. Quant. Chem. 100 (2004) 834.
[50] G.L. Yudin, A.D. Bandrauk, P.B. Corkum, Phys. Rev. Lett. 96 (2006) 063002.